IJHSR
ijhighschoolresearch.org
RESEARCH ARTICLE

Simulating Hatchet Oar Blade Motion Using SnappyHexMesh and Turbulence Modeling in OpenFOAM

Sean Schwartz

Episcopal High School, 1200 N. Quaker Ln, Alexandria, VA, 22302, USA; seanschwartzshs@gmail.com

ABSTRACT: This work models the hydrodynamics of the blade of a rower by means of computational fluid dynamics in the open-source software OpenFOAM, wherein simulations were carried out on a convex hatchet oar geometry at various blade angles (-20˚ to +20˚) to study the pressure distribution, wake formation, and force coefficients, using a blockMesh generated computational domain, steady simulations with simpleFoam. The results show that a 0˚ blade angle results in the highest total force (Cd=1.7994) due to an optimum pressure differential-wake coherence balance, and so is the most efficient blade-angle for a rower to maintain throughout the middle of the stroke. An entrance angle of approximately -20˚ was found to minimize drag, which indicates an efficiency of a catch/Entry angle of -20˚ before inevitable rotation toward 0˚ during the drive. The results present a computational basis for blade shape and kinematics optimization in rowing propulsion.

KEYWORDS: Computational Fluid Dynamics, Rowing Blade, OpenFOAM, Rowing Propulsion, Turbulence Modeling.

Introduction

At the heart of rowing propulsion is a moving blade and a moving fluid, each pushing and yielding to the other. Describing that exchange: how force becomes motion, how motion disturbs the water, how the nature of the flow creates velocity and pressure, is the job of the Navier–Stokes equations.[1] It accounts for how velocity changes not just over time, but over space: how a fluid speeds up, how it shears, how it spreads or narrows or decelerates. In rowing, that happens along the blade surface, in the pressure gradients that it creates, and in the vortices that it creates behind it. The essence is this: fluid momentum is altered by forces within—viscosity, pressure, and inertia. Water near the blade sticks to it; it slows down, swirls around, and stratifies. Water farther away reacts to those changes. Near the surface, thin layers form where velocity gradients are greatest—boundary layers, sensitive to blade angle and motion.[2] Further away, the bulk flow curves and becomes vortices, especially at the edges.[3] All of it is regulated by the same principles, contained in the same equations.

Since water can't be compressed to any significant degree at these speeds, conservation of volume necessitates that fluid that enters some location must leave from somewhere else. That necessity—what mathematicians call "divergence-free"—along with the pressure and velocity fields, binds them together tightly.[1] You can't change one without affecting the other. What makes the system difficult to solve—and interesting to study—is its nonlinearity. Water doesn't simply respond to forces; it transmits them. A whirling blade doesn't simply disturb water at the moment it passes; it changes the way the next moment will be. That feedback is what makes rowing propulsion more than a simple cause-and-effect system. The same laws and equations of Fluid dynamics govern hurricanes, airplane wings, and ink spreading through water.[4] But in rowing, the environment is small, the conditions are more localized, and the results are more immediate. Each stroke is an in-the-moment experiment in unsteady flow.[5]

Turbulence occurs when the orderly patterns of flow break down into layers of uncertainty: when viscosity is overcome by inertia, and small perturbations are no longer damped, but amplified.[4] In rowing, this happens around and behind the blade, where flow is separated, sheared, and careened into vortices. These vortices, formed at the blade edges, possess momentum and energy, marking the edge between smooth pressure-driven motion and the complex, swirling aftermath. As they interact and stretch, some remain coherent, others break into smaller eddies, cascading energy downwards through scales.[3] This process is set by equations, but is also effectively impossible to do by hand, thus requiring computational modeling or experiment to mark the edge between the elegant and the chaotic in each stroke.

These vortices also influence the unsteady pressure field and create fluctuations in lift and drag. The stroke efficiency is not only a matter of blade speed and angle, but of whether or not these vortices are stable and attached, or detach randomly into the wake. This is where lift and drag coefficients, Cl and Cd, enter the picture. They describe how effectively the blade is converting motion into force, and they change with blade angle, flow separation, and formation of vortices.[4] A small change in angle or speed will make the flow go from smooth and efficient to turbulent and wasteful. Understanding how these coefficients respond to blade geometry and stroke kinematics is the key to developing an efficient propulsion system.[5] This paper aims to incorporate the described factors to simulate and determine the optimal blade angles in terms of pressure, force, and turbulence for different moments throughout the stroke.

DOI: 10.36838/IJHSR811.249

Methods

The simulations were carried out with OpenFOAM (version 11), an open-source CFD package. The computational domain was generated with blockMesh. A large rectangular domain was produced to minimize boundary effects. A simplified convex hatchet oar blade was inserted into this domain and turned to discrete angles between -20° and +20°.

The following boundary conditions were implemented in OpenFOAM to simulate realistic water flow around the blade.

The numerical domain used inlet velocity boundary conditions on the lower face (Z = -0.5) in modeling blade motion in water. Zero-gradient pressure boundary conditions on the upper outlet (Z = +0.5) modeled natural wake development. Symmetry boundary conditions on the side, front, and back faces minimized computational expense and removed edge effects in modeling the infinite span flow behavior of the blade.

The necessary Oar blade geometries were generated from a Python script that generates STL files by tilt angle, starting from a definition of a 2D oar shape with realistic cleaver-blade size (500 mm long, 250 mm wide). A cambered surface shape is defined by a parabolic thickness distribution with a 10mm maximum camber in a 2mm base thickness. The 2D shape was then triangulated by Delaunay triangulation, then extruded to form top and bottom surfaces connected by vertical side walls. The geometry was lastly rotated around the centre point to make the tilt angle (-20° to 20° at discrete steps), and the resulting triangular mesh was saved as a watertight STL file ready for CFD simulation.

The final computational mesh was created with the OpenFOAM snappyHexMesh utility, which refines arches and surfaces automatically. This utility works through three separate stages:

Stage 1: Castellated Mesh Creation

- Surface refinement levels were used to properly follow the blade's surface geometry
- Refinement boxes were created around the blade to guarantee proper resolution in the wake region
- Maximum refinement level: 4 (cell size = background_cell_size / 2^4)
- Minimum refinement level: 3 (for base resolution)

Stage 2: Surface Snapping

- Castellated mesh was snapped to match the STL surface geometry of the oar blade
- Feature edge refinement was used to capture sharp edges and corners
- Surface normal smoothing iterations: 3
- Tolerance settings optimized to preserve geometric quality

Stage 3: Boundary Layer Addition

- Prismatic boundary layer cells were added next to the blade surface
- First layer thickness: 0.3 (relative to local cell size)
- Number of boundary layers: 3
- Growth ratio: 1.2
- Total boundary layer thickness: ~0.93 (relative units)

The numerical model is based on the discretization of the Navier–Stokes equations in OpenFOAM using the finite volume method.[1] These equations are expressed in a conservative form for mass and momentum:

$$\nabla \cdot u = 0$$

$$\partial u/\partial t + (u \cdot \nabla)u = - (1/\rho) \nabla p + \nu \nabla^2 u$$

where u is velocity, p is pressure, ρ is fluid density, and ν is kinematic viscosity.

Steady-state simulations were performed initially with simpleFoam to validate mesh quality, numerical stability, and boundary conditions.[7] The turbulence model used was k–ω SST, known to model correctly flow separation and vortex transport phenomena, which are of importance for the rowing blade performance.[8]

Upon validation, the blade was rotated up to each specified angle in increments, and simulations were performed until the force coefficients obtained converged. The results of the simulations included the time average of the drag and lift coefficients (Cd and Cl) and of the moment coefficient (Cm). The coefficients were found by performing surface integrals of the pressure and viscous stresses on the blade using the solver.[4] The velocity and pressure fields were exported at each step and visualized using ParaView-5.13.3. Within ParaView, there could be detailed observation of wake structures, pressure gradients, and isolated flow separation zones for the various simulated blade angles. In the future, there are plans to incorporate unsteady simulations using the features pimpleFoam and dynamicsMesh into the simulation in order to emulate real rowing more closely.

Results and Discussion

To assess the hydrodynamic performances of a rowing blade at different pitch angles, several steady state simulations have been carried out by simpleFoam in OpenFOAM. The blade shape was a basic convex hatchet profile within a large computational space to reduce edge effects. Simulations were performed for blade angles of –20° up to +20° in 5° steps. For each case, pressure and velocity field monitoring, aerodynamic coefficients extraction, and flow structure visualization in ParaView were performed.

The main quantities to be studied were the drag coefficient (Cd), the lift coefficient (Cl), the moment coefficient (Cm), and the magnitude of resulting forces. These were derived at each angle and processed to find the best arrangements for mounting propulsion and for stability and entry. Some important highlights:

$$F = (1/2)\, \rho\, C_A\, A\, v^2$$

where:

- $p = 1000\ kg/m^3$ (density of water)
- C_A = coefficient of lift (Cl) or drag (Cd)
- $A = 0.125\ m^2$ (cross-sectional area of the blade: 0.5m × 0.25m)
- $v^2 = 2\ m/s$ (velocity of the blade through water)

From that equation, the drag and lift forces were extracted via OpenFOAM from the surface pressure. Then the forces

were normalized by the dynamic pressure (1/2pv^2) and reference area.

$C_d = F_d / ((1/2)\rho v^2 A)$

$C_l = F_l / ((1/2)\rho v^2 A)$

Maximum Drag Configuration (Best for Power Transfer):
- Blade Angle: 0°
- Drag Coefficient (Cd): 1.7994
- Lift Coefficient (Cl): -0.0005
- Total Force Magnitude: 1.7994

Maximum Lift Configuration (Lateral Stability):
- Blade Angle: 15°
- Drag Coefficient (Cd): 1.6922
- Lift Coefficient (Cl): -0.0020
- Total Force Magnitude: 1.6922

Minimum Drag Configuration (Blade Entry/Catch Phase):
- Blade Angle: -20°
- Drag Coefficient (Cd): 1.5563

Maximum Total Force Configuration (Overall Propulsion):
- Blade Angle: 0°
- Same as Max Drag Configuration

Table 1: Force Coefficient Results.

Angle (°)	Cd	Cl	Cm
-20	1.5563	-0.0012	-0.0209
-15	1.6442	-0.0018	-0.0204
-10	1.7225	-0.0016	-0.0219
-5	1.7757	-0.0013	-0.0225
0	1.7994	-0.0005	-0.0229
5	1.7797	-0.0014	-0.0211
10	1.7582	-0.0016	-0.0206
15	1.6922	-0.0020	-0.0186
20	1.5939	-0.0014	-0.0182

Table 1 shows a complete distribution of how such coefficients change with blade angle. Both net force and drag coefficient can be modeled with a negative parabola with a vertex peak at 0° and equal negative rate of change in either direction to the ends of 20° or -20°. This parabolic result trend with a peak at 0° proves that the mid-stroke blade position plays a large role in thrust generation. These results align with the pressure field indicated in Figure 2: the 0° blade angle displays a high-pressure front and has a consistent low-pressure wake.

As expected, the lift coefficient was negative for all tested angles (from -20° to 20°), given that the blades face downwards relative to the flow. Another indication of the relative believability of these results is the incredibly small ratio between lift forces and drag forces for all angles. However, the relatively small amount of lift coefficient does not invalidate its role within the stroke, as it is an important contributor to stroke stability through lateral corrections. Figure 4 most directly illustrates how the lift force is always smaller than the drag force by an order of magnitude, supporting the conclusion that drag plays the largest role in rowing propulsion.

Similar to the lift coefficient, the moment coefficient is negative for all angles. As the angle increases from -20 to 20, so does the moment coefficient. These results are similar to those of steady torque, which is generated by asymmetrical pressure distribution, therefore indicating the influence of the moment coefficient on handle control and force.

Velocity and pressure field visualizations (Figures 2 and 3) show strong wake formation and pressure gradients around the blade surfaces. At 0°, the blade created a clean downstream wake with mirrored high-pressure buildup on the leading surface and low-pressure trailing wake. In positive angles larger than 0°, stronger wake regions and further downstream flow separation on the blade were observed with increased inefficiency. Such flow characteristics are in direct relation to the decrease of the total force with angle, as seen in Figure 1.

Such regimes of wake turbulence and flow separation, as existing, could be related to the calculation of the Reynolds number. The Reynolds number for this case analysis has been computed by the application of the relative water velocity (U = 2m/s) together with the chord length of the blade (c = 0.5m):

$Re = \rho Uc/\mu = (1000 \times 2 \times 0.5) / (1\times10^{-3}) = 1\times10^{6}$

This supercritical Reynolds number possesses fully turbulent flows with the current boundary layer transition and the strong wake. The positive blade angles (> 0°) for the turbulent wake indicate the separation of the flows within the adverse pressure gradients, sufficient to overcome the boundary layer momentum, as clearly visible from the velocity field visualisations for +15° and +20°.

For $Re = 1\times10^{6}$, the boundary layer switches automatically to turbulent flow near the leading edge, producing the high wake formation and pressure gradients observed in Figures 2 and 3. The 0° wake characteristic showed attached turbulent flow with late separation, but the presence of turbulence with increasing positive angle shows boundary layer separation early along the suction side of the blade due to the adverse pressure gradient. In the RANS simulation, there was no wake turbulence present at the angle of simulation, perhaps an indication of the favorable pressure gradients. Wake turbulence was not observed for the -20° angle of attack in the present steady RANS simulation, suggesting favorable pressure gradients that may delay boundary layer separation. The absence of turbulence at -20 degrees could also have been influenced by the boundary conditions encoded in the implementation of the steady RANS simulation.

At –20°, where the drag force is minimized in the Drag Coefficient vs Blade Angle graph (Figure 1), would be the op-

DOI: 10.36838/IJHSR811.249

timal position for blade entry to maintain a smooth entrance. In a simulation that aims to maximize net turbulence of the stroke, a minimized entry turbulence may seem unintuitive. However, the compromise is optimized to allow angle entry with a smaller resistive load without overtly compromising the boat's acceleration downstream.

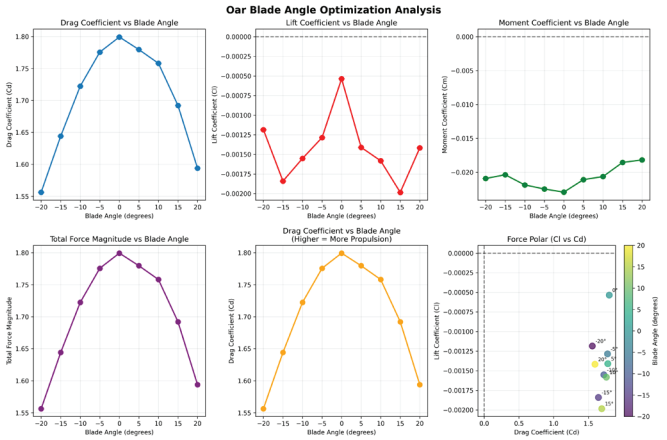

Figure 1: Oar Blade Angle Optimization Analysis Graphs. Simulation post-analysis graphs of Cd, Cl, Cm, and total force magnitude with blade angle from −20° to +20°: displaying a parabolic dependence, resulting in maximum drag and total force at 0°, and minimized drag at −20°.

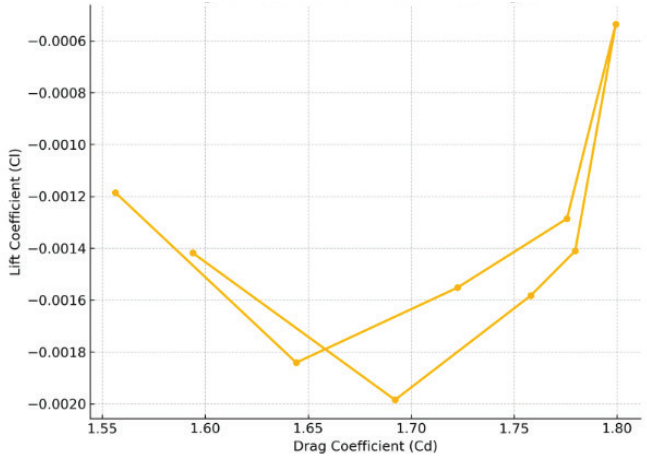

Figure 2: Cd vs Cl for Different Blade Angels.

Within shows two lines; each point represents the increase in blade angle from -20° to 0° and the decrease from 20° to 0°. Given how similar these lines are, it confirms the parabolic relationship between Cd/Cl and the blade angles.

Conclusion

This study determined that, given a steady-state water condition, the blade angle that will generate the maximum net force is 0°. The steady-state condition describes the rower in the middle of the stroke post-entry, where he seeks to simply maximize propulsion. However, for other periods of the stroke, the rower is inclined to compromise. When the rower places their blade into the water, doing so with the maximum drag would disrupt the velocity and smooth glide of the boat. The simulated angle of 20° had the minimized drag force, allowing for a less disruptive and resistive blade entry. Therefore, the entry angle of 20° followed by an instant rotation into 0° would maintain the boat's smooth glide and allow for an undisruptive acceleration as the blade engages with maximum drag throughout the rest of the stroke.

The OpenFOAM code used to produce the hydrodynamic blade simulations can be found along with a CSV dataset of force and moment coefficients.

(https://github.com/NecritsSoup/OpenFOAM-simulation)

Further research is considered, as these files provide a framework for more unsteady simulations as well as implications for rowing analysis and equipment development.

Acknowledgments

I would like to thank my mentor, Adam Almakroudi, for guiding me through the literature and tools required for this research.

I attest that the ideas, graphics, and writing in this paper are entirely my own.

References

1. Batchelor GK. *An Introduction to Fluid Dynamics*. Cambridge: Cambridge University Press; 2000. Eldredge JD, Jones AR. Leading-edge vortices: mechanics and modeling. *Annu Rev Fluid Mech* 2019;51:75–104.
2. Sujono S, Saputra E, Ismail R. Analysis of oar blade hydrodynamics for rowing propulsive mechanism: experiment and computational fluid dynamics simulation. *CFD Lett* 2019;11(3):112–123.
3. Bardina JE, Huang PG, Coakley TJ. *Turbulence Modeling Validation, Testing, and Development*. NASA Technical Memorandum 110446. Moffett Field, CA: NASA Ames Research Center; 1997.
4. Schlichting H, Gersten H. *Boundary-Layer Theory*. 9th ed. Berlin: Springer; 2017.
5. Weller HG, Tabor G, Jasak H, Fureby C. A tensorial approach to computational continuum mechanics using object-oriented techniques. *Comput Phys* 1998;12(6):620–631.
6. Menter FR. Two-equation eddy-viscosity turbulence models for engineering applications. *AIAA J* 1994;32(8):1598–1605.
7. Grift EJ, Tummers MJ, Westerweel J. Hydrodynamics of rowing propulsion. *J Fluid Mech* 2021;918:A29.
8. White FM. *Fluid Mechanics*. 8th ed. New York: McGraw-Hill Education; 2016.

Author

Sean Schwartz is a senior at Episcopal High School. He spends a great deal of time rowing, playing the piano, and playing cello in his school orchestra. Drawing on his experience as a varsity rower and his interest in computational modeling, Sean has undertaken several research projects related to fluid dynamics and oar blade propulsion.